

# High-threshold fault-tolerant quantum computation with the GKP qubit and realistically noisy devices

Kosuke Fukui

*Department of Applied Physics,  
School of Engineering, The University of Tokyo,  
7-3-1 Hongo, Bunkyo-ku, Tokyo 113-8656, Japan*

To implement fault-tolerant quantum computation with continuous variables, continuous variables need to be digitized using an appropriate code such as the Gottesman–Kitaev–Preskill (GKP) qubit. We have developed a method to alleviate the required squeezing level to realize fault-tolerant quantum computation with the GKP qubit [K. Fukui, A. Tomita, A. Okamoto, and K. Fujii, *Phys. Rev. X* **8**, 021054 (2018)]. In the previous work, the required squeezing level can be reduced to less than 10 dB, assuming a noise derived from only the deviation of the GKP qubit itself. Considering realistic devices such as the two-qubit gate and the homodyne measurement, however, there is some additional noise, which leads to the degradation of the squeezing level. Specifically, the required squeezing level degrades to 15.0 dB, assuming the transmission loss in the homodyne measurement 5 % and the imperfection of the two-qubit gate. In this work, we propose a scheme to improve the required squeezing level, combining the previous schemes with the proposed maximum-likelihood methods and encoded measurements. The numerical calculations show that the required squeezing levels are 8.3, 9.6, and 11.7 dB for the transmission loss in the homodyne measurement 0, 5, and 10 %, respectively, considering the imperfection of the two-qubit gate. Hence, we believe this work will open up a new way to implement continuous-variable fault-tolerant quantum computation with a moderate squeezing level and realistically noisy devices.

## I. INTRODUCTION

Quantum computation (QC) has a great deal of potential to efficiently solve some hard problems for conventional computers [1, 2]. To realize large-scale QC, the continuous variable (CV) system is a promising platform; in fact, more than one million-mode 1-dimensional cluster state composed of the squeezed vacuum states has been experimentally generated in an optical setup [3]. Nowadays, a 2-dimensional cluster state for a computation depth of about 5,000 modes on 5 inputs has been generated [4]. Soon after their work, a 2-dimensional cluster state for a computation depth of 1250 modes on 24 inputs has been generated [5]. Furthermore, more than thousands of a frequency-encoded cluster state in an optical set up has been generated [6–8]. In addition to an optical setup, the CV system a circuit QED [9], opto-mechanics [10, 11], atomic ensembles [12, 13], and a trapped ion mechanical oscillator [14, 15] are also promising candidates for large-scale QC with CVs.

Regarding fault-tolerant QC (FTQC) with CVs (CV-FTQC), it is known that CVs need to be digitized using an appropriate code, such as a cat code, a binomial code, or the Gottesman–Kitaev–Preskill (GKP) code [16] referred to as the GKP qubit in this work. This is because the squeezed vacuum state can not handle the accumulation of analog errors, for example, e.g. the Gaussian quantum channel [16] and a photon loss during the quantum computation. In 2014, Menicucci for the first time showed the threshold of required squeezing level for the CV-FTQC for measurement-based QC [17], where the GKP qubit is used to implement the quantum error correction during.

Recently, there have been many efforts to towards FTQC with the GKP qubit [18–22], and a promising architecture for a scalable quantum circuit incorporating the GKP qubit [23, 24]. In our previous work [18], we have proposed a high-

threshold FTQC with the GKP qubits to alleviate the required squeezing level for CV-FTQC to 9.8 dB, which is within the reach of the current experimental technology [25]. For the noise model in Ref. [18], however, we have considered only the deviation derived from the GKP qubit itself, where the deviations propagate between the GKP qubits by the two-qubit gate. Still, considering realistic devices, there is some additional noise such as that derived from the imperfection of the two-qubit gate and the homodyne measurement, which leads to the degradation of the squeezing level. Then, it is naturally expected to degrade the threshold value of the squeezing level, which means that there is a large gap between the experimentally achievable squeezing level and the theoretical requirement.

In this work, we devise a scheme to achieve a further reduction of the required squeezing level for CV-FTQC under the realistic assumption for the two-qubit gate and the homodyne measurement, developing the method to implement the highly-reliable construction of the large-scale cluster state by harnessing analog information contained in the GKP qubits. Specifically, our method consists of two parts. One is to make use of the Gauss-Markov theorem, which is widely known in statistics, to reduce a noise of the GKP qubits in the construction of the small scale cluster state. The other is the reliable deterministic entanglement generation to obtain the large scale cluster state, where we select the most reliable entanglement generation by using a maximum-likelihood method. Accordingly, the required squeezing level for CV-FTQC using the proposed method can be reduced to 8.3 and 9.6 dB for the transmission loss in the homodyne measurement  $l = 0$  and 5 %, respectively, while those using the previous method are 10.7 and 15.0 dB, respectively, assuming the imperfection of the two-qubit gate. Furthermore, our method enables us to implement topologically protected MBQC with 11.7 dB for  $l = 10$  %, while topologically protected MBQC using the previ-

ous method is impossible with more than  $l \sim 7.8\%$ .

The rest of the paper is organized as follows. In Sec. II, we briefly review the background knowledge regarding the GKP qubit, and the realistically noisy devices considered in this work. In Sec. III, we propose the method to reduce the required squeezing level for CV-FTQC with the realistically noisy devices. In Sec. IV, the numerical results show the superiority of the proposed method over the conventional methods. Section V is devoted to discussion and conclusion.

## II. GKP QUBIT AND REALISTICALLY NOISY DEVICES

### A. The GKP qubit

Gottesman, Kitaev, and Preskill proposed a method to encode a qubit in an oscillator's  $q$  (position) and  $p$  (momentum) quadratures to correct errors caused by a small deviation in the  $q$  and  $p$  quadratures [16]. The basis of the GKP qubit is composed of a series of Gaussian peaks of width  $\sigma$  and separation  $\sqrt{\pi}$  embedded in a larger Gaussian envelope of width  $1/\sigma$ . Although in the case of infinite squeezing ( $\sigma \rightarrow 0$ ) the GKP qubit bases become orthogonal, in the case of finite squeezing, the approximate code states are not orthogonal. The approximate code states  $|\tilde{0}\rangle$  and  $|\tilde{1}\rangle$  are defined as

$$|\tilde{0}\rangle \propto \sum_{t=-\infty}^{\infty} \int e^{-2\pi\sigma^2 t^2} e^{-(q-2t\sqrt{\pi})^2/(2\sigma^2)} |q\rangle dq, \quad (1)$$

$$|\tilde{1}\rangle \propto \sum_{t=-\infty}^{\infty} \int e^{-\pi\sigma^2(2t+1)^2/2} e^{-(q-(2t+1)\sqrt{\pi})^2/(2\sigma^2)} |q\rangle dq. \quad (2)$$

In the case of the finite squeezing, there is a finite probability of misidentifying  $|\tilde{0}\rangle$  as  $|\tilde{1}\rangle$ , and vice versa. Provided the magnitude of the true deviation is more than  $\sqrt{\pi}/2$  from the peak value, the decision of the bit value is incorrect. The probability  $E(\sigma^2)$  of misidentifying the bit value is calculated by

$$E(\sigma^2) = 1 - \int_{-\frac{\sqrt{\pi}}{2}}^{\frac{\sqrt{\pi}}{2}} dx \frac{1}{\sqrt{2\pi\sigma^2}} \exp\left(-\frac{x^2}{2\sigma^2}\right). \quad (3)$$

### B. Realistically noisy devices

In this work, we assume two noisy devices, specifically the imperfection of the two-qubit gate and the homodyne measurement. For the noisy two-qubit gate, we consider the CNOT gate demonstrated in Ref. [26, 27], which is called as the QND gate [26, 27]. In the QND gate, the interaction between the control qubit C and the target qubit T is implemented by using a beam-splitter coupling with two squeezed vacuum states A and B. The QND gate with the reflectivity of the beam splitter  $R$  and the squeezing parameters  $r_A$  and  $r_B$

for squeezed vacuum states transforms as

$$\hat{q}_C \rightarrow \hat{q}_C - \sqrt{\frac{1-R}{1+R}} \hat{q}_A e^{-r_A}, \quad (4)$$

$$\hat{p}_C \rightarrow \hat{p}_C - \frac{1-R}{\sqrt{R}} \hat{p}_T + \sqrt{\frac{R(1-R)}{1+R}} \hat{p}_B e^{-r_B}, \quad (5)$$

$$\hat{q}_T \rightarrow \frac{1-R}{\sqrt{R}} \hat{q}_C + \hat{q}_T + \sqrt{\frac{R(1-R)}{1+R}} \hat{q}_A e^{-r_A}, \quad (6)$$

$$\hat{p}_T \rightarrow \hat{p}_T + \sqrt{\frac{1-R}{1+R}} \hat{p}_B e^{-r_B}, \quad (7)$$

where  $\hat{q}_C(\hat{p}_C)$ ,  $\hat{q}_T(\hat{p}_T)$ ,  $\hat{q}_A(\hat{p}_A)$ , and  $\hat{q}_B(\hat{p}_B)$  are the quadrature operators of the control qubit, target qubit, and two squeezed vacuum states in the  $q(p)$ , respectively. In the case that the coefficient  $(1-R)/\sqrt{R}$  is equal to 1 and the squeezing level of squeezed vacuum states are infinite, the QND gate is equivalent to the ideal CNOT gate, which corresponds to the operator  $\exp(-i\hat{q}_A\hat{p}_D)$ . Regarding the variance of the GKP qubit, the QND gate changes the variances of the control and target qubits as

$$\sigma_{C,q}^2 \rightarrow \sigma_{C,q}^2 + \frac{1-R}{1+R} \sigma_A^2, \quad (8)$$

$$\sigma_{C,p}^2 \rightarrow \sigma_{C,p}^2 + \frac{(1-R)^2}{R} \sigma_{C,p}^2 + \frac{R(1-R)}{1+R} \sigma_B^2, \quad (9)$$

$$\sigma_{T,q}^2 \rightarrow \sigma_{C,q}^2 + \frac{(1-R)^2}{R} \sigma_{T,q}^2 + \frac{R(1-R)}{1+R} \sigma_A^2, \quad (10)$$

$$\sigma_{T,p}^2 \rightarrow \sigma_{T,p}^2 + \frac{1-R}{1+R} \sigma_B^2, \quad (11)$$

where variances  $\sigma_{C,q(p)}^2$  and  $\sigma_{T,q(p)}^2$  are the variances of the control qubit and the target qubit in the  $q(p)$  quadrature, respectively. In this work, we assume that  $\sigma_A^2$  and  $\sigma_B^2$  are equal to  $\sigma_{SV}^2$ , where variances  $\sigma_A^2$  and  $\sigma_B^2$  are the variances of two squeezed vacuum states A and B. In this paper, we set the squeezing level of the squeezed vacuum used for the QND gate to 15 dB, which is the currently achievable squeezing level[28]. For the noisy CZ gate, the QND gate is equivalent to the CZ gate up to local Fourier transformations.

Secondly, we consider the imperfection of the homodyne measurement by using a model of a transmission loss before the homodyne detector. This model can be formulated by placing beam splitters before the homodyne detector, where the input state couples with a vacuum state by a beam splitter. The transmission loss transforms the variables in the  $q$  and  $p$  quadratures as

$$\hat{q} \rightarrow \sqrt{\eta} \hat{q}, \quad \hat{p} \rightarrow \sqrt{\eta} \hat{p}, \quad (12)$$

where  $\sqrt{\eta}$  is the transmittance coefficient of a beam splitter. The variance of the input state in the  $q(p)$  quadrature,  $\sigma_{in,q(p)}^2$ , changes as,

$$\sigma_{in,q(p)}^2 \rightarrow \sigma_{out,q(p)}^2 = \eta \sigma_{in,q(p)}^2 + \frac{1-\eta}{2}. \quad (13)$$

The probability to misidentify the bit value after the transmission loss in the  $q(p)$  quadrature is calculated by

$E(\sigma_{\text{out},q(p)}^2/\eta)$  in Eq. (3). Note that the variance  $\sigma_{\text{out},q(p)}^2$  is modified in order to calculate the probability of misidentifying the bit value as

$$\sigma_{\text{out},q(p)}^2 \rightarrow \frac{\sigma_{\text{out},q(p)}^2}{\eta} = \sigma_{\text{in},q(p)}^2 + \frac{1-\eta}{2\eta}, \quad (14)$$

where we multiply the outcome of the homodyne measurement by  $1/\sqrt{\eta}$  in classical post-processing to fix the basis of the GKP qubit at the integer multiples of  $\sqrt{\pi}$ .

### III. HIGH-THRESHOLD FTQC WITH REALISTICALLY NOISY DEVICES

#### A. Cluster state construction with the ME-SQEC

In this subsection, we describe the single-qubit level quantum error correction (SQEC) with a maximum-likelihood estimation (ME-SQEC), and explain the method to generate the 3-tree cluster with a low error accumulation. The 3-tree cluster is used to construct the hexagonal cluster with encoded qubits, as described in the next subsection.

The SQEC is has been proposed to correct a displacement (deviation) error [16]. In the ME-SQEC, the SQEC is used to estimate the true deviation value of the GKP qubit by using the maximum-likelihood estimation. In the conventional SQEC in the  $p$  quadrature, an additional qubit prepared in the state  $|\tilde{0}\rangle$  is entangled with the data qubit as the ancilla by the CNOT gate, where the data and ancilla qubits are the target and control qubits, respectively. The CNOT gate, which corresponds to the operator  $\exp(-i\hat{q}_a\hat{p}_D)$  for continuous variables, transforms the true deviation values in the  $p$  quadrature as

$$\bar{\Delta}_{p,a} \rightarrow \bar{\Delta}_{p,a} - \bar{\Delta}_{p,D}, \quad \bar{\Delta}_{q,D} \rightarrow \bar{\Delta}_{q,D} + \bar{\Delta}_{q,a}, \quad (15)$$

where  $\bar{\Delta}_{q,D}$  ( $\bar{\Delta}_{p,D}$ ) and  $\bar{\Delta}_{q,a}$  ( $\bar{\Delta}_{p,a}$ ) are the true deviation values of the data and ancilla qubits in the  $q$  and  $p$  quadratures, respectively. We assume that the variances of the data (ancilla) qubit in the  $q$  and  $p$  quadratures are  $\sigma_{\text{D(a)},q}^2$  and  $\sigma_{\text{D(a)},p}^2$ , respectively, and for simplicity, the CNOT gate is ideal. From the measurement outcome, we obtain the deviation of the ancilla  $\Delta_{mp,a} = p_k + \Delta_{mp,a}$  to minimize the deviation  $|\Delta_{mp,a}|$ , where  $p_k$  ( $k = 0, 1$ ) is defined as  $(2t+k)\sqrt{\pi}$  ( $t = 0, \pm 1, \pm 2, \dots$ ). Then, we perform the displacement  $|\Delta_{mp,a}|$  on the data qubit in the  $p$  quadrature to minimize the true deviation. If  $|\bar{\Delta}_{p,a} - \bar{\Delta}_{p,D}|$  is less than  $\sqrt{\pi}/2$ , the true deviation value of the data qubit in the  $p$  quadrature changes to  $\bar{\Delta}_{p,a}$ , which displaces  $\bar{\Delta}_{p,D}$  by  $\Delta_{mp,a}$  ( $= \bar{\Delta}_{p,a} - \bar{\Delta}_{p,D}$ ). On the other hand, if  $|\bar{\Delta}_{p,a} - \bar{\Delta}_{p,D}|$  is more than  $\sqrt{\pi}/2$ , the bit error in the  $p$  quadrature occurs. As a consequence, the SQEC for the data qubit in the  $p$  quadrature can reduce the variance of the data qubit in the  $p$  quadrature from  $\sigma_{\text{D},p}^2$  to  $\sigma_{a,p}^2$ . The variance of the data qubit in the  $q$  quadrature after the SQEC increases from  $\sigma_{\text{D},q}^2$  to  $\sigma_{\text{D},q}^2 + \sigma_{a,q}^2$  (see also Appendix A for the SQEC in the  $p$  quadrature).

In the ME-SQEC, we estimate the true deviation of the data qubit by considering the Gauss-Markov theorem that is widely

known in statics. For the SQEC with the Gauss-Markov theorem, the true deviation of the data qubit is estimated by the ancilla qubit, where the maximum-likelihood estimation is based on the fact that the true deviation values are obeyed the Gaussian distribution independently. In the ME-SQEC in the  $q$  quadrature, as a result of the measurement of the qubit A after the CZ gate between the data qubit D and ancilla qubit A, the true deviation of the qubit D obeys posterior probability that is Gaussian distribution of mean:

$$\delta = \frac{\sigma_{q,D}^2}{\sigma_{q,D}^2 + \sigma_{p,A}^2} (\bar{\Delta}_{p,A} - \bar{\Delta}_{q,D}) \quad (16)$$

with the variance

$$\sigma_{q,D}'^2 = \frac{\sigma_{q,D}^2 \sigma_{p,A}^2}{\sigma_{q,D}^2 + \sigma_{p,A}^2}. \quad (17)$$

By performing the displacement operation to the data qubit by  $\delta$ , the variance of the qubit D in  $q$  quadrature reduces from  $\sigma_{p,A}^2$  to  $\sigma_{q,D}'^2$ , while the variance in  $p$  quadrature increases from  $\sigma_{p,D}^2$  to  $\sigma_{p,D}^2 + \sigma_{q,A}^2$ . In the case where  $\sigma_{p,D}^2 = \sigma_{q,A}^2 = \sigma^2$ , the ME-SQEC improves the variance of the data qubit in the  $q$  quadrature by  $\sigma^2/2$  in comparison to the SQEC without a maximum-likelihood estimation [31]. (see also [32] for a very recent and a related method regarding the improvement of the variance using the maximum-likelihood estimation in the single-qubit level.) We note that while the variance of the GKP qubit reduces by using the ME-SQEC, the qubit level error occurs, if the deviation value is more than  $\sqrt{\pi}/2$  and the misidentification of the bit value occurs. To reduce the probability of misidentifying the bit value of the ancilla, we use the highly reliable measurement (HRM) introduced in Ref. [18]. (see also Appendix B for the description of the HRM.)

We move on to the preparation of the 3-tree cluster with a low error accumulation by using ME-SQEC with the HRM. As shown in Fig. 1(a), the entangled two qubits is generated using the CZ gate between the two single qubits. After the CZ gate, the variances of the two qubits are  $\sigma^2$  and  $2\sigma^2$  in the  $q$  and  $p$  quadratures, respectively, where the variances of the single qubit in the  $q$  and  $p$  are  $\sigma^2$ . Then, we reduce the variances of the two qubits in the  $q$  and  $p$  quadratures by repeatedly and independently applying the ME-SQEC with the HRM to the each of entangled two qubits (Fig. 1(b)). In the ME-SQEC in the  $p$  ( $q$ ) quadrature, the node and leaf qubits are the control (target) qubits, where the ancilla qubits are prepared in  $|\tilde{0}\rangle$  ( $|\tilde{+}\rangle$ ). In the ME-SQEC, the HRM reduces the probability of misidentifying the bit value of the ancilla used for estimating the variances. After the generation of the reliable entangled two qubits, we construct the 3-tree cluster using the CZ gate between the single qubit and one of the entangled two qubits (Fig. 1(c)). In a similar way as the generation of the entangled two qubits, the variances of the node qubit and one of the leaf qubits in the  $q$  and  $p$  quadratures are reduced, as shown in Fig. 1(d). Accordingly, we can obtain the 3-tree cluster state with a low error accumulation. Although we can reduce the variances of the 3-tree cluster to be close to  $\sigma^2$  with the ideal two-qubit gate and the homodyne

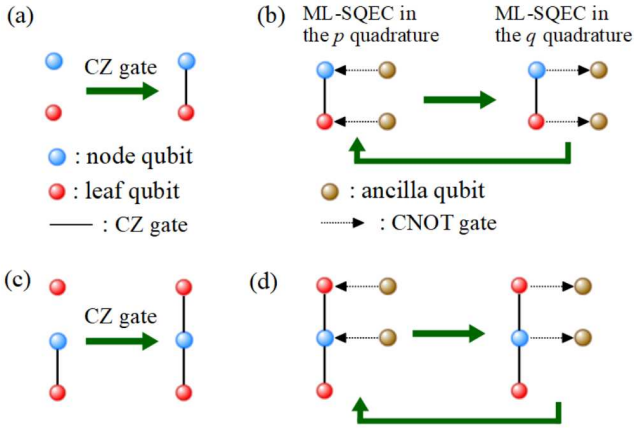


FIG. 1. The preparation of the 3-tree cluster with the ME-SQEC with the highly reliable measurement (HRM). (a) The generation of the entangled two qubits using the CZ gate. (b) The construction of entangled two qubits with a low error accumulation, repeatedly applying the ME-SQEC in the  $q$  and  $p$  quadratures, where ancilla qubits prepared in  $|\pm\rangle$  and  $|0\rangle$  are the target and control qubit, respectively. (c) The generation of the entangled 3-tree cluster from the single qubit and the entangled two qubits using the CZ gate. (d) The construction of the 3-tree cluster with a low error accumulation, repeatedly applying the ME-SQEC in the  $q$  and  $p$  quadratures.

measurement, we should stop the iteration of the ME-SQEC due to the qubit level errors in the ME-SQEC with the HRM. In the numerical simulation, the number of iterations of the ME-SQEC in the  $q$  and  $p$  quadratures is set to 3.

## B. Construction of the 3D cluster

In the previous work [18], we proposed the reliable construction of 3D cluster, where the fusion gate with the HRM is used to avoid the error accumulation during the construction of the hexagonal cluster as shown in Fig. 2(a). In this work, we apply the encoded hexagonal cluster and reliable deterministic generation of the 3D cluster to the reliable construction of 3D cluster. The encoded hexagonal cluster as shown in Fig. 2(b), which consists of six node qubits and  $2L$  encoded leaf qubits per one of the node qubits, is constructed from the 3-tree cluster prepared using the ME-SQEC. In the deterministic generation of the 3D cluster, the reliable fusion gate is implemented thanks to the encoded measurement using encoded leaf qubits, where the maximum-likelihood method and the repetition code reduce the error probability in the fusion gate. In the following, we explain the construction of the 3D cluster, where there are three steps, as shown in Fig. 2(c)-(i).

In step 1, we prepare the 3-tree cluster using the ME-SQEC with the HRM, as described in the previous subsection. In step 2, we construct the hexagonal cluster states with the encoded leaf qubits from the 3-tree cluster state, as shown in Fig. 2(c)-(f). In this step, we use the fusion gate with the HRM in the same manner as described in Ref. [18], where the Bell measurement is used to maintain the variance of the node qubit, and the HRM is used to reduce the failure proba-

bility derived from misidentifying the bit value in the fusion gate. Specifically, the 4-tree cluster is constructed from two 3-tree clusters, and the 5-tree cluster is constructed from the 3-tree cluster and the 4-tree cluster by using the Bell measurement with the HRM (Fig. 2(c)). The encoded 3-tree cluster is constructed from four 5-tree clusters (Fig. 2(d)), and the encoded 5-tree cluster (Fig. 2(e)) is obtained from the two encoded 3-tree clusters and the 5-tree cluster by using the fusion gate with the HRM. We then obtain the hexagonal cluster states with the encoded leaf qubits (Fig. 2(b)) from six encoded 5-tree clusters. Because of the HRM in steps 1 and 2, the highly-reliable cluster is obtained with a low error accumulation at the cost of the success probability of the HRM.

In step 3, the 3D cluster is constructed from the hexagonal clusters by using the deterministic fusion gate without the HRM. In this step, the HRM can not be used to obtain the 3D cluster, because the 3D cluster needs to be constructed deterministically to perform large scale QC deterministically. In the conventional method [18], the deterministic generation between two nodes is implemented by the Bell measurement on the two leaf qubits of each of the two hexagonal clusters. Since the error probability of the fusion gate without the HRM is several orders of magnitude higher than that with the HRM, the error probability of the deterministic fusion gate is the bottleneck for the threshold of the squeezing. In this work, we propose the encoded measurement with a maximum-likelihood method to reduce the error probability of the deterministic fusion gate.

In the proposed fusion gate without the HRM, we first implement the Bell measurement between the two leaf qubits of each of the two hexagonal clusters as shown in Fig. 2(g). After all Bell measurements, we then select the most reliable entanglement by using the maximum-likelihood method, comparing  $L$  likelihoods for measurement results. We here assume that we obtain the  $i$ -the measurement deviation  $\Delta_{m,Ai}$  and  $\Delta_{m,Bi}$  are obtained from the  $i$ -the Bell measurement on the two  $i$ -the leaf qubits connected with the node qubit. The  $i$ -the likelihood is calculated by

$$F_i = f(\Delta_{m,Ai})f(\Delta_{m,Bi}), \quad (18)$$

where  $f(x)$  is the Gaussian distribution function with mean zero and variance  $\sigma_{\text{pro},q}^2 + \sigma_{\text{pro},p}^2$ , and  $\sigma_{\text{pro},q}^2$  and  $\sigma_{\text{pro},p}^2$  are the variances of the leaf qubit in the  $q$  and  $p$  quadratures, respectively. We next select the measurement result that has the largest likelihood as the measurement result for the most reliable entanglement. We then keep the most reliable entanglement by the measurement on the ancillae, while we remove the entanglement except for the most reliable one. For the most reliable entanglement, we measure the ancillae connected with the most reliable entanglement in the  $q$  quadrature in order to remove the ancillae from the entanglement, as shown in Fig. 2(h). The ancillae are safely removed, since the probability of misidentifying the bit value in the  $q$  quadrature is sufficiently small compared with that in the  $p$  quadrature. This is because we end up with the ME-SQEC in the  $q$  quadrature to reduce the variance of the ancilla qubit, which means that the variance of the ancilla qubit in the  $q$  quadrature is smaller than that in the  $p$  quadrature. For the entanglement

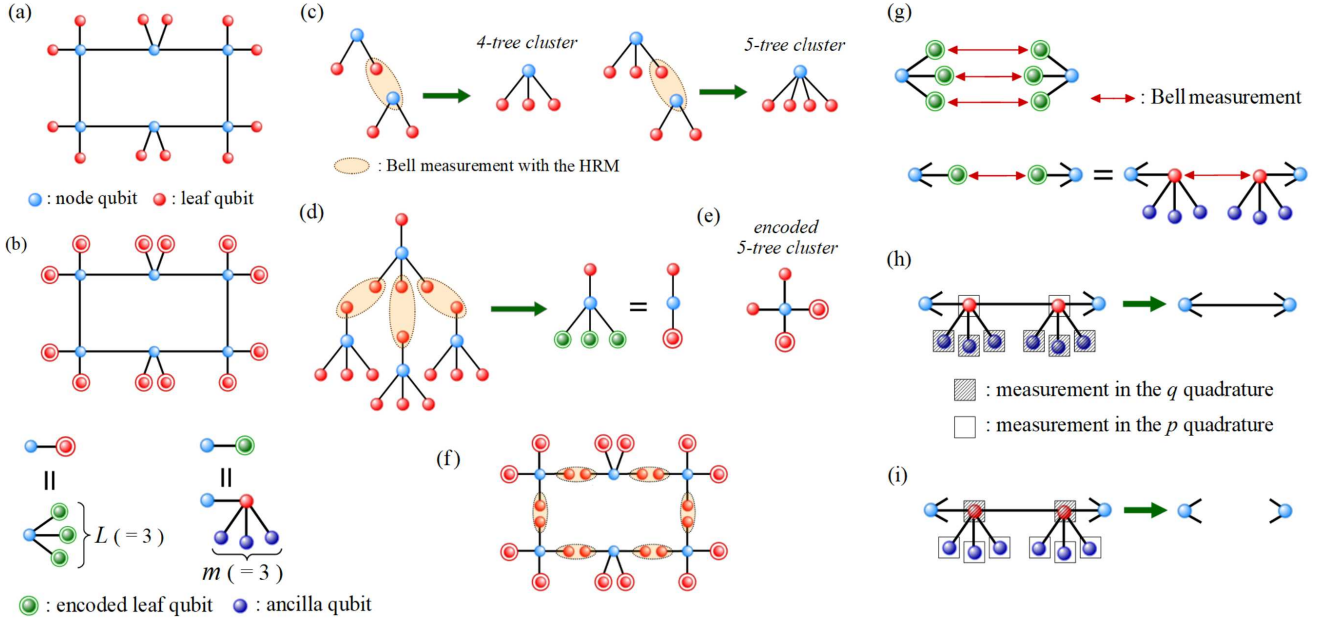


FIG. 2. The 3D cluster construction. (a) The hexagonal cluster introduced in Ref.[18]. (b) The hexagonal cluster with the encoded leaf qubits, where the number of the encoded leaf qubits and ancilla qubits composing each of the encoded leaf qubit are  $L(=3)$  and  $m(=3)$ , respectively. (c) The construction of the 4-tree cluster and 5-tree cluster from the 3-tree clusters. (d) The construction of the encoded 3-tree cluster from four 5-tree clusters. (e) The encoded 5-tree cluster, which is constructed from the 5-tree cluster and two encoded 3-tree cluster. (f) The construction of the hexagonal cluster with the encoded leaf qubits from six encoded 5-tree clusters. (g) The Bell measurement between the two leaf qubits connected with each of nodes, where the measurement is implemented without the HRM. (h) The measurement on the ancillae in the  $q$  quadrature for the most reliable entanglement. (i) The measurement on the ancillae in the  $p$  quadrature for the entanglement except for the most reliable entanglement.

except for the most reliable entanglement, we measure the ancillae in the  $p$  quadrature so that we obtain the bit value of the leaf qubit in the  $q$  quadrature, as shown in Fig. 2(i). We accurately obtain the bit value of the leaf qubit, and safely remove the entanglement between nodes and ancillae thanks to the encoded measurement, where ancillae are encoded by them-repetition code in the  $p$  quadrature. In the  $m$ -repetition code for the encoded leaf qubit, the node qubit  $N$  and the  $i$ -th ancilla qubit  $A_i$  are stabilized by the operator

$$\hat{Z}_N \hat{X}_{A_i} = +1 \quad (i = 1, 2, \dots, m), \quad (19)$$

where  $m$  is the number of ancillae, and we implement a majority voting among the measurement results of ancillae in the  $p$  quadrature. For instance, we decide that the bit value of the node qubit in the  $q$  quadrature is 0 by using a majority voting, when the measurement results of ancillae with  $m = 3$  are  $\hat{X}_{A_1} = +1$ ,  $\hat{X}_{A_2} = +1$ , and  $\hat{X}_{A_3} = -1$ , respectively, namely, we obtain the bit values of the ancillae in the  $p$  quadrature as 0, 0, and 1, respectively. This type of the indirect measurement, which obtains the bit value indirectly from the measurements of ancillae, was introduced by Varnava *et al.* [29]. Furthermore, in our method, the analog QEC [30] is employed to enhance the QEC performance of the repetition code. Consequently, we can obtain the 3D cluster with a low error accumulation by using the deterministic fusion gate with encoded leaf qubits and the construction of the hexagonal cluster with a maximum-likelihood method.

#### IV. THRESHOLD CALCULATION

In this section, for simplicity, we estimate the threshold value of the squeezing level required for the CV-FTQC by using the conventional [18] and proposed methods, assuming the imperfection of the QND gate and the homodyne measurement. Later, we take a more detailed calculation by the numerical simulation of the QEC for topologically protected MBQC. In this calculation, we set the upper limit  $v_{up}$  for the HRM to  $2\sqrt{\pi}/5$ , and the number of iterations of the ME-SQEC in the preparation of the 3-tree cluster to 3 for each of quadratures.

In the conventional method [18], where the topologically protected MBQC is performed on the highly-reliable 3D cluster, the threshold value in the leading order is calculated by using the probability  $E_{tot}$  that is the unheralded error probability per one node qubit of the 3D cluster in the  $p$  quadrature. In Ref. [18],  $E_{tot}$  in the leading order is obtained by

$$E_{tot} = E_{node} + E_{HRM} + 2E_{det}, \quad (20)$$

where  $E_{node}$  is the probability of misidentifying the bit value of the node qubit,  $E_{HRM}$  is the sum of the probabilities of misidentifying the bit value in the fusion gate with the HRM during the construction of the hexagonal cluster, and  $E_{det}$  is the probability of misidentifying the bit value in the deterministic fusion gate without HRM. Since  $E_{node}$ ,  $E_{HRM}$  are sufficiently small under the condition of the upper limit



$v_{\text{up}} = 2\sqrt{\pi}/5$  for the HRM,  $E_{\text{tot}}$  can be approximated by  $2E_{\text{det}} = 2E(\sigma'^2)$ , where the variance  $\sigma'^2$  is derived from the sum of the variance of the leaf qubit in the  $q$  and  $p$  quadratures. The probability  $E(\sigma'^2)$  is calculated by Eq.(3) up to the replacement of  $\sigma^2$  by  $\sigma'^2$ . Then, we define the threshold value of the squeezing level as the squeezing level that provides  $E_{\text{tot}} = 2E(\sigma'^2) = 3\%$ , which is the threshold value for topologically protected MBQC 2.9 – 3.3% [33, 34]. To estimate the threshold value for the realistic noisy devices with the conventional method [18], we calculate  $\sigma'^2$  as

$$\sigma'^2 = 3\sigma^2 + \sigma_{\text{sv}}^2(1-R) + \frac{1-\eta}{2\eta}, \quad (21)$$

where  $\sigma_{\text{sv}}^2$  is the variance of the squeezed vacuum in the QND gate and  $R$  is  $(3 - \sqrt{5})/2$  corresponding to  $(1-R)/\sqrt{R} = 1$  in Eqs.(5) and (6). By using the previous method without the analog QEC, we obtain the threshold in the leading order 11.6, 14.2, and 17.9 for the transmission loss rate in the homodyne measurement  $l = 0, 3, \text{ and } 5\%$ , respectively, assuming the squeezing level of the squeezed vacuum state is 15.0 dB in the QND gate, where  $1-l$  corresponds to the transmission coefficient  $\eta$ . Furthermore, we find that topologically protected MBQC without the analog QEC is impossible more than  $l \sim 6.4\%$ , even when the GKP qubit has an infinite squeezing level. This is because the variance derived from the sum of the loss and the squeezed vacuum state in the QND gate is equal to the variance corresponding to the  $E_{\text{tot}} = 3\%$ .

In the proposed method using the hexagonal cluster with the encoded leaf qubits, instead of the  $E_{\text{det}}$ , we consider the probabilities  $E_{\text{det,pro}}$  for the deterministic fusion gate with our scheme. Then, the total probability with the proposed method  $E_{\text{tot,pro}}$  in the leading order is calculated by

$$E_{\text{tot,pro}} = E_{\text{node}} + E_{\text{HRM}} + 2E_{\text{det,pro}}. \quad (22)$$

$E_{\text{det,pro}}$  consists of the probabilities  $E_{\text{ML}}$ ,  $E_{\text{anc,q}}$ , and  $E_{\text{anc,p}}$ , where  $E_{\text{ML}}$  is the probability of the misidentification of the bit value of the leaf qubit for the most reliable entanglement, the  $E_{\text{anc,q}}$  is the probability of the misidentification of the bit value of the ancilla qubits connected with the most reliable entanglement, and the  $E_{\text{anc,p}}$  is the failure probability of the repetition code to remove the entanglement with the node qubit. Specifically,  $E_{\text{det,pro}}$  is described by

$$E_{\text{det,pro}} = E_{\text{ML}} + mE_{\text{anc,q}} + (L-1)E_{\text{anc,p}}, \quad (23)$$

where  $L$  is a half of the number of the leaf qubits per one of the node qubits, and  $m$  is the number of the ancilla qubit connected with each of the leaf qubits. Since  $E_{\text{node}}$ ,  $E_{\text{HRM}}$ , and  $E_{\text{anc,q}}$  are sufficiently small,  $E_{\text{tot}}$  can be approximated by

$$E_{\text{tot}} \sim 2E_{\text{ML}} + 2(L-1)E_{\text{anc,p}}. \quad (24)$$

Additionally, the probability  $E_{\text{anc,p}}$ , which is the failure probability of the  $m$ -repetition code for odd  $m$ , is calculated in the leading order as

$$E_{\text{anc,p}} \sim m C_{\frac{m-1}{2}} E(\sigma_{\text{pro}}^2)^{\frac{m-1}{2}}, \quad (25)$$

where  $\sigma_{\text{pro}}^2$  is the variance derived from the sum of the variance of the leaf qubit in the  $q$  and  $p$  quadratures. The variance  $\sigma_{\text{pro}}^2$  is described as  $\sigma_{\text{pro}}^2 = \sigma_{\text{pro,q}}^2 + \sigma_{\text{pro,p}}^2 + (1-\eta)/2\eta$ . Accordingly, the proposed method can reduce the threshold of squeezing level compared with the previous method, if  $E_{\text{tot,pro}}$  is smaller than  $E_{\text{tot}}$ . For the numerical calculation in the leading order, we set the number of the leaf qubits  $L$  and ancillae  $m$  to 4 and 3, respectively. Then, for simplicity, we regard estimate  $E_{\text{det}}$  to be the probability of misidentifying the bit value using the HRM with the upper limit  $v_{\text{up}} = 2\sqrt{\pi}/5$  whose value provides the success probability 99.9 % for the entanglement generation with  $L = 4$ . Consequently, we find that the threshold value without the analog QEC are 8.9, 10.2, and 12.1 dB in the leading order with the transmission loss rate  $l = 0, 5, \text{ and } 10\%$ , respectively, assuming that the squeezing level of the squeezed vacuum state is 15.0 dB in the QND gate. We note that this calculation in the leading order with the proposed method is potentially inaccurate, since the deterministic fusion gate to construct the 3D cluster is substituted by the

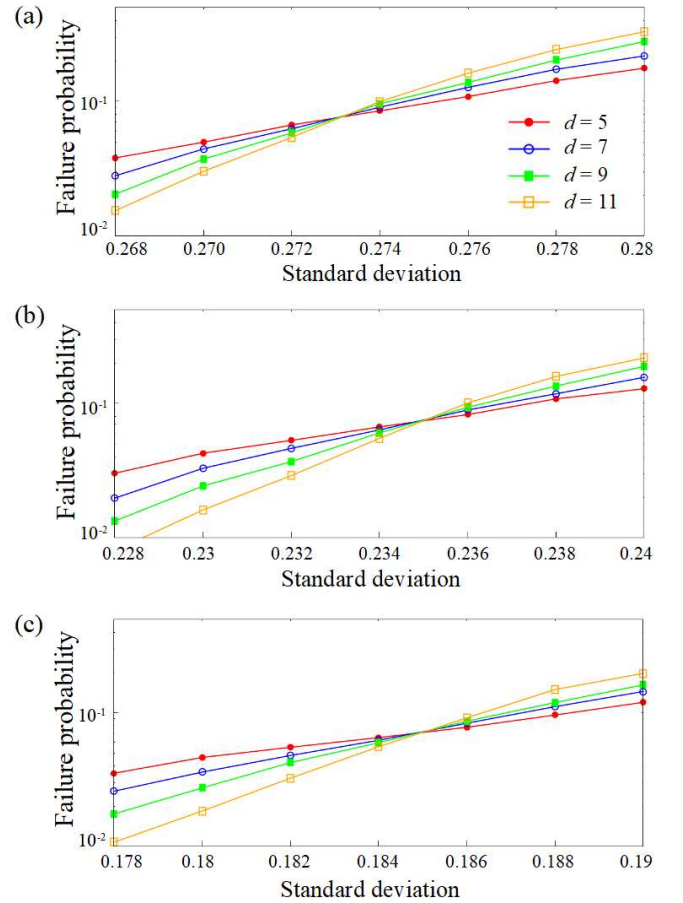


FIG. 3. Simulation results for the failure probabilities of the QEC of the surface code with the analog QEC for the transmission loss  $l =$  (a) 0%, (b) 5%, and (c) 10%, respectively, are plotted as a function of the standard deviation of the GKP qubits for the code distances  $d = 5, 7, 9, \text{ and } 11$ . The QEC process is simulated by using the 3D cluster prepared by the proposed method with  $v_{\text{up}} = 2\sqrt{\pi}/5$ . The simulation results are obtained from 10000 samples.

non-deterministic fusion gate with the HRM.

To proceed a detailed calculation with the analog QEC, we numerically simulate the QEC process for topologically protected MBQC by using the minimum-weight perfect-matching algorithm [35, 36] for the code distances  $d = 5, 7, 9$ , and 11. In this simulation, we apply the analog QEC[30] to improve the QEC performance of the surface code in topologically protected MBQC and the repetition code in the deterministic fusion gate. In Fig. 3, the logical error probabilities are plotted as a function of the standard deviation of the GKP qubit for  $l = 0\%$ ,  $5\%$ , and  $10\%$ , which corresponds to  $\eta = 1.0, 0.95$ , and  $0.9$ . The numerical results confirm that our method for  $l = 0, 5$ , and  $10\%$  achieves the threshold value of the standard deviation  $0.273, 0.235$ , and  $0.185$ , which correspond to the threshold value of the squeezing level  $8.3, 9.6$ , and  $11.7$  dB, respectively. The squeezing level  $s$  is equal to  $s = -10\log(2 \times \sigma^2)$ , where the variance  $\sigma$  is the standard deviation of the GKP qubit. Moreover, we numerically simulate the QEC process for topologically protected MBQC using the previous method with the analog QEC. Numerical results shows that the threshold values are  $10.7$  and  $15.0$  for  $l = 0$  and  $5\%$ , respectively, assuming the squeezing level of the squeezed vacuum state is  $15.0$  in the QND gate. In addition, we find that topologically protected MBQC with the analog QEC is impossible more than  $l \sim 7.8\%$ , even when the GKP qubit has an infinite squeezing level. Therefore, the threshold of the squeezing level with the conventional method degrades by  $\sim 5.4$  dB compared with the previous method.

## V. DISCUSSION AND CONCLUSION

In this work, we have developed the method to improve the squeezing level required for FTQC with the GKP qubit under the realistic noisy devices, where the two-qubit gate and the homodyne measurement are imperfect. In our method, we have proposed a maximum-likelihood method to reduce a noise of the GKP qubits in the SQEC and the deterministic fusion gate with the encoded measurement, and combined the proposed methods with the conventional high-threshold FTQC [18]. The numerical calculations have shown that the required squeezing level can be improved to less than  $10$  dB with analog QEC up to about the transmission loss in the homodyne measurement  $5\%$ , which is will be able to generate with the near-term experimental set-up [25], while topologically protected MBQC with the previous method is impossible with the around  $10$  dB. Furthermore, our method enables us to CV-FTQC with  $11.7$  dB for the transmission loss  $10\%$ , while topologically protected MBQC using the previous method is impossible. Hence, we believe this work will open up a new way to implement CV-FTQC with a moderate squeezing level under the realistic setup.

Future works could look at a noise model derived from the imperfection during the generation of the GKP qubit. Such a noise model has been studied in Refs. [19, 37] focusing the breeding protocol, while the threshold of the squeezing level with the analog QEC schemes has not been obtained in the noise model. We could calculate the threshold of squeez-

ing level for CV-FTQC by using in this work, considering the noise derived from the generation of the GKP qubit.

## ACKNOWLEDGEMENTS

KF thanks Keisuke Fujii for for useful discussions.

## Appendix A: Single-qubit level QEC

After the SQEC in the  $p$  quadrature, the SQEC in the  $q$  quadrature can be performed using the second ancilla, where the ancilla is prepared in the state  $|\tilde{+}\rangle$  and the data qubit is assumed to be the control qubit. Regarding the deviation, the CNOT gate operation displaces the deviation of the  $q$  and  $p$  quadratures as

$$\bar{\Delta}_{q,a2} \rightarrow \bar{\Delta}_{q,a2} + \bar{\Delta}_{q,D} + \bar{\Delta}_{q,a}, \quad (\text{A1})$$

$$\bar{\Delta}_{p,a2} \rightarrow \bar{\Delta}_{p,a2}, \quad (\text{A2})$$

$$\bar{\Delta}_{q,D} + \bar{\Delta}_{q,a} \rightarrow \bar{\Delta}_{q,D} + \bar{\Delta}_{q,a}, \quad (\text{A3})$$

$$\bar{\Delta}_{p,a} \rightarrow \bar{\Delta}_{p,a} - \bar{\Delta}_{p,a2}, \quad (\text{A4})$$

where  $\bar{\Delta}_{q,a2}(\bar{\Delta}_{p,a2})$  is the true deviation value of the second ancilla in the  $q$  ( $p$ ) quadrature. After the CNOT gate, we measure the ancilla in the  $q$  quadrature, and obtain the deviation of the ancilla  $\Delta_{mq,a2}$ . Then, we perform the displacement  $|\Delta_{mq,a2}|$  on the  $q$  quadrature of the data qubit to correct by shifting back in the direction to minimize the deviation. If  $|\Delta_{mq,a2}| = |\bar{\Delta}_{q,a2} + \bar{\Delta}_{q,D} + \bar{\Delta}_{q,a}|$  is less than  $\sqrt{\pi}/2$ , the true deviation value of the data qubit in the  $q$  quadrature changes from  $\bar{\Delta}_{q,D} + \bar{\Delta}_{q,a}$  to  $-\bar{\Delta}_{q,a2}$  after the displacement operation, which displaces  $\bar{\Delta}_{q,D} + \bar{\Delta}_{q,a}$  by  $-\Delta_{mp,a} (= -\bar{\Delta}_{q,a2} - \bar{\Delta}_{q,D} - \bar{\Delta}_{q,a})$ . On the other hand, if  $|\Delta_{mq,a2}|$  is more than  $\sqrt{\pi}/2$ , the bit error in the  $q$  quadrature occurs after the displacement operation. To summarize, after the sequential SQECs in the  $p$  and  $q$  quadrature, the variances of the data qubit in the  $q$  and  $p$  quadratures become  $\sigma_{a,q}^2$  and  $2\sigma_{a,p}^2$ , respectively. Although the SQEC works well for the small deviation, we need to operate the logical-qubit level QEC to correct the deviation greater than  $\sqrt{\pi}/2$ .

## Appendix B: Highly-reliable measurement

The HRM can reduce the probability of misidentifying the bit value of the GKP qubit by introducing upper limit  $v_{up}$  as a decision line of the bit value. In the conventional measurement, the decision sets an upper limit for  $|\Delta_m|$  at  $\sqrt{\pi}/2$ , and assigns the bit value  $k = (2t + k)\sqrt{\pi}$ , as shown in Fig. 4 (a). In the HRM, the decision sets an upper limit at  $v_{up} (< \sqrt{\pi}/2)$  to give the maximum deviation that will not cause incorrect measurement of the bit value as shown in Fig. 4. If the above condition  $|\Delta_m| < v_{up}$  is not satisfied, we discard the result. Since the measurement error occurs when  $|\bar{\Delta}|$  exceeds  $|\sqrt{\pi}/2 + v_{up}|$ , the error probability decreases as increasing  $v_{up}$  at the cost of the success probability of the measurement. The probability

to obtain the correct bit value with the HRM  $P_{\text{post}}$  is equal to  $P_{\text{post}}^{\text{cor}}/(P_{\text{post}}^{\text{cor}} + P_{\text{post}}^{\text{in}})$ , where  $P_{\text{post}}^{\text{cor}}$  is the probability that the true deviation  $|\bar{\Delta}|$  falls in the correct area, and  $P_{\text{post}}^{\text{in}}$  is the probability that the true deviation  $|\bar{\Delta}|$  falls in the incorrect area.  $P_{\text{post}}^{\text{cor}}$  and  $P_{\text{post}}^{\text{in}}$  for the GKP qubit of the variance  $\sigma^2$  are given by

$$P_{\text{post}}^{\text{cor}} = \sum_{k=-\infty}^{+\infty} \int_{2k\sqrt{\pi} - \frac{\sqrt{\pi}}{2} + v_{\text{up}}}^{2(k+1)\sqrt{\pi} + \frac{\sqrt{\pi}}{2} - v_{\text{up}}} dx \frac{1}{\sqrt{2\pi\sigma^2}} e^{-\frac{x^2}{2\sigma^2}} \quad (\text{B1})$$

and

$$P_{\text{post}}^{\text{in}} = \sum_{k=-\infty}^{+\infty} \int_{(2k+1)\sqrt{\pi} - \frac{\sqrt{\pi}}{2} + v_{\text{up}}}^{(2k+1)\sqrt{\pi} + \frac{\sqrt{\pi}}{2} - v_{\text{up}}} dx \frac{1}{\sqrt{2\pi\sigma^2}} e^{-\frac{x^2}{2\sigma^2}}. \quad (\text{B2})$$

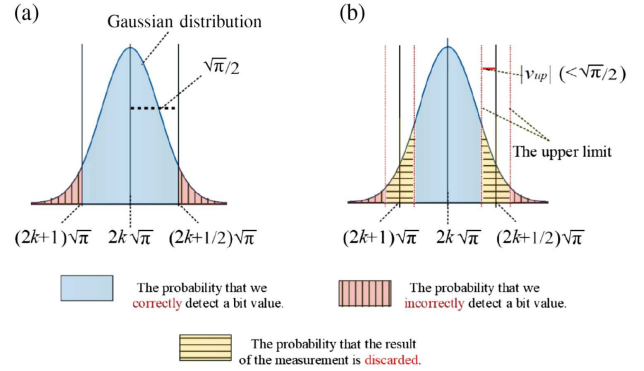


FIG. 4. Introduction of the highly-reliable measurement. (a) The conventional measurement of the GKP qubit, where the Gaussian distribution followed by the deviation of the GKP qubit that has variance  $\sigma^2$ . The plain (blue) region and the region with vertical (red) line represent the different code word  $(k-1) \bmod 2$  and  $(k+1) \bmod 2$ , respectively. The vertical line regions correspond to the probability of incorrect decision of the bit value. (b) The highly-reliable measurement. The shown dot line represents an upper limit  $v_{\text{up}}$ . The horizontal line areas show the probability that the results of the measurement is discarded by introducing  $v_{\text{up}}$ . The vertical line areas show the probability that our method fails.

- 
- [1] P. W. Shor, Polynomial-Time Algorithms for Prime Factorization and Discrete Logarithms on a Quantum Computer, *SIAM J. Comp.* **26**, 1484 (1997).
- [2] L. K. Grover, Quantum Mechanics Helps in Searching for a Needle in a Haystack, *Phys. Rev. Lett.* **79**, 325 (1997).
- [3] J. Yoshikawa, S. Yokoyama, T. Kaji, C. Sornphiphatphong, Y. Shiozawa, K. Makino, and A. Furusawa, Generation of one-million-mode continuous-variable cluster state by unlimited time-domain multiplexing, *APL Photonics* **1** 060801 (2016).
- [4] W. Asavanant, Y. Shiozawa, S. Yokoyama, B. Charoensombutamon, H. Emura, R. N. Alexander, S. Takeda, J. Yoshikawa, N. C. Menicucci, H. Yonezawa, and A. Furusawa, Time-Domain Multiplexed 2-Dimensional Cluster State: Universal Quantum Computing Platform, arXiv:1903.03918.
- [5] M. V. Larsen, X. Guo, C. R. Breum, J. S. Neergaard-Nielsen, and U. L. Andersen, Deterministic generation of a two-dimensional cluster state for universal quantum computing, arXiv:1906.08709.
- [6] M. Pysher, Y. Miwa, R. Shahrokhshahi, R. Bloomer, and O. Pfister, Parallel Generation of Quadripartite Cluster Entanglement in the Optical Frequency Comb, *Phys. Rev. Lett.* **107**, 030505 (2011).
- [7] M. Chen, N. C. Menicucci, and O. Pfister, Experimental Realization of Multipartite Entanglement of 60 Modes of a Quantum Optical Frequency Comb, *Phys. Rev. Lett.* **112**, 120505 (2014).
- [8] J. Roslund, R. M. Araújo, S. Jiang, C. Fabre, and N. Treps, Wavelength-Multiplexed Quantum Networks with Ultrafast Frequency Combs, *Nature Photonics*, **8**, 109-112 (2014).
- [9] A. L. Grimsmo, A. Blais, Squeezing, and Quantum State Engineering with Josephson Travelling Wave Amplifiers, *npj Quantum Information*, **3**, 20 (2017).
- [10] M. Schmidt, M. Ludwig, and F. Marquardt, Optomechanical Circuits for Nanomechanical Continuous Variable Quantum State Processing, *New J. Phys.* **14**, 125005 (2012).
- [11] O. Houhou, H. Aissaoui, and Alessandro Ferraro, Generation of Cluster States in Optomechanical Quantum Systems, *Phys. Rev. A* **92**, 063843 (2015).
- [12] Y. Ikeda and N. Yamamoto, Deterministic Generation of Gaussian Pure States in a Quasilocal Dissipative System, *Phys. Rev. A* **87**, 033802 (2013).
- [13] K. R. Motes, B. Q. Baragiola, A. Gilchrist, and N. C. Menicucci, Encoding Qubits into Oscillators with Atomic Ensembles and Squeezed Light, *Phys. Rev. A* **95**, 053819 (2017).
- [14] C. Flühmann, V. Negnevitsky, M. Marinelli, and J. P. Home, Sequential Modular Position and Momentum Measurements of a Trapped Ion Mechanical Oscillator, *Phys. Rev. X* **8**, 021001 (2018).
- [15] C. Flühmann, T. L. Nguyen, M. Marinelli, V. Negnevitsky, K. Mehta, and J. P. Home, Encoding a Qubit in a Trapped-ion Mechanical Oscillator, *Nature* **566**, 513-517 (2019).
- [16] D. Gottesman, A. Kitaev, and J. Preskill, Encoding a qubit in an oscillator, *Phys. Rev. A* **64**, 012310 (2001).
- [17] N. C. Menicucci, Fault-Tolerant Measurement-Based Quantum Computing with Continuous-Variable Cluster States, *Phys. Rev. Lett.* **112**, 120504 (2014).
- [18] K. Fukui, A. Tomita, A. Okamoto, and K. Fujii, *Phys. Rev. X*



- 8, 021054 (2018).
- [19] T. Douce, D. Markham, E. Kashefi, P. van Loock, and G. Ferrini, Probabilistic fault-tolerant universal quantum computation and sampling problems in continuous variables, *Phys. Rev. A* **99**, 012344 (2019).
- [20] C. Vuillot, H. Asasi, Y. Wang, L. P. Pryadko, and B. M. Terhal, Quantum Error Correction with The Toric Gottesman-Kitaev-Preskill Code, *Phys. Rev. A* **99**, 032344 (2019).
- [21] B. Q. Baragiola, G. Pantaleoni, R. N. Alexander, A. Karanjai, and N. C. Menicucci, All-Gaussian Universality and Fault Tolerance with the Gottesman-Kitaev-Preskill Code, arXiv:1903.00012.
- [22] B. W. Walshe, L.J. Mensen, B. Q. Baragiola, and N. C. Menicucci, Robust Fault Tolerance for Continuous-Variable Cluster States with Excess Anti-Squeezing, arXiv:1903.02162.
- [23] S. Takeda and A. Furusawa, Universal Quantum Computing with Measurement-Induced Continuous-Variable Gate Sequence in a Loop-Based Architecture, *Phys. Rev. Lett.* **119**, 120504 (2017).
- [24] R. N. Alexander, S. Yokoyama, A. Furusawa, and N. C. Menicucci, Universal Quantum Computation with Temporal-Mode Bilayer Square Lattices, *Phys. Rev. A* **97**, 032302 (2018).
- [25] B. M. Terhal and D. Weigand, Encoding a Qubit into a Cavity Mode in Circuit QED Using Phase Estimation, *Phys. Rev. A* **93**, 012315 (2016).
- [26] J. Yoshikawa, Y. Miwa, A. Huck, U. L. Andersen, P. van Loock, A. Furusawa, Demonstration of a Quantum Nondemolition Sum Gate, *Phys. Rev. Lett.* **101**, 250501 (2008).
- [27] Y. Shiozawa, J. Yoshikawa, S. Yokoyama, T. Kaji, K. Makino, T. Serikawa, R. Nakamura, S. Suzuki, S. Yamazaki, W. Asavanant, S. Takeda, P. van Loock, and A. Furusawa, Quantum Nondemolition Gate Operations and Measurements in Real Time on Fluctuating Signals, *Phys. Rev. A* **98**, 052311 (2019).
- [28] H. Vahlbruch, M. Mehmet, K. Danzmann, and R. Schnabel, Detection of 15 dB Squeezed States of Light and Their Application for The Absolute Calibration of Photoelectric Quantum Efficiency, *Phys. Rev. Lett.* **117**, 110801 (2016).
- [29] M. Varnava, D. E. Browne, and T. Rudolph, in One-Way Quantum Computation via Counterfactual Error Correction, *Phys. Rev. Lett.* **97**, 120501 (2006).
- [30] K. Fukui and A. Tomita and A. Okamoto, Analog Quantum Error Correction with Encoding a Qubit into an Oscillator, *Phys. Rev. Lett.* **119**, 180507 (2017).
- [31] In the case of the estimation of the deviation value  $\bar{\Delta}_{q,D}$  using  $n$  ancillae with  $\sigma_{p,D}^2 = \sigma_{q,A}^2 = \sigma^2$ , after measurement of  $n$  ancillae in  $p$  quadrature, we obtain the deviation value  $\bar{\Delta}_{p,A_i} - \bar{\Delta}_{q,D}$ . Then, we can estimate the deviation value  $\bar{\Delta}_{q,A}$  as  $(\sum_{i=1}^n \bar{\Delta}_{p,A_i} - \bar{\Delta}_{q,D})/(n+1)$ , by using the maximum-likelihood estimation. As a result, the variance of the qubit A in  $q$  quadrature reduces from  $\sigma^2$  to  $\sigma^2/(n+1)$ , while the variance of the qubit A in  $p$  quadrature increases from  $\sigma^2$  to  $(n+1)\sigma^2$ .
- [32] K. Noh, S. M. Girvin, and L. Jiang, Encoding an oscillator into many oscillators, arXiv:1903.12615.
- [33] C. Wang, J. Harrington, and J. Preskill, Confinement-Higgs transition in a disordered gauge theory and the accuracy threshold for quantum memory, *Ann. Phys.* **303**, 31 (2003).
- [34] T. Ohno, G. Arakawa, I. Ichinose, and T. Matsui, Phase structure of the random-plaquette gauge model: accuracy threshold for a toric quantum memory, *Nucl. Phys. B* **697**, 462 (2004).
- [35] J. Edmonds, Paths, trees, and flowers, *Canadian Journal of mathematics* **17**, 449 (1965).
- [36] V. Kolmogorov, Blossom v: a new implementation of a minimum cost perfect matching algorithm, *Mathematical Programming Computation* **1**, 43 (2009).
- [37] Y. Shi, C. Chamberland, and A. W. Cross, Fault-Tolerant Preparation of Approximate GKP States, arXiv:1905.00903.